

First-principles study of the atomic reconstructions of ZnSe(100) surfaces

C. H. Park and D. J. Chadi

NEC Research Institute, 4 Independence Way, Princeton, New Jersey 08540

(Received 18 January 1994)

We examine the reconstructions and surface energies of ZnSe(100) surfaces by first-principles total-energy calculations. The surface energies for the Zn- and Se-terminated (1×1) , (1×2) , (2×1) , (2×2) , and Zn-terminated (4×2) reconstructed surfaces consisting of various combinations of dimers and vacancies are determined as a function of coverage and atomic chemical potential. For the Zn- and Se-terminated surfaces, dimerization lowers the energies by 2.12 and 1.08 eV per dimer, respectively. When exchange with bulk Zn or Se reservoirs is considered, a $c(2 \times 2)$ Zn-vacancy structure is found to be energetically more favorable than a dimer structure for the Zn-terminated surface, while a (2×1) dimer structure is the most favorable one for the Se-terminated surface.

I. INTRODUCTION

Recently, there has been a great deal of interest in wide-band-gap II-VI semiconductors. In particular, ZnSe is being actively studied as a result of recent successes in the fabrication of blue-light-emitting laser diodes.^{1,2} However, the problem of heavy *p*-type doping (in the $10^{19}/\text{cm}^3$ range) still remains unsolved for ZnSe and other II-VI sulfides and selenides.³ Surface structure is important in the understanding of growth and impurity incorporation mechanisms. First-principles total-energy methods have been successfully applied to the study of the semiconductor surface reconstructions, and provide a powerful tool for understanding the energetics of various defect formations and surface reconstructions. These calculations have been performed mostly for Si (Refs. 4–8) and GaAs surface;^{9–14} the reconstructions of II-VI semiconductor surface have not yet been examined.

Experimentally, a $c(2 \times 2)$ periodicity for the Zn-terminated surface and a (2×1) reconstruction for the Se-terminated (100) surface have been seen.^{15–19} No other types of structures have been observed. Menda, Minato, and Kawashima used reflection-high-energy electron diffraction to study the surface reconstructions during the (100) homoepitaxial growth as a function of the vapor pressure ratio $P_{\text{Se}}/P_{\text{Zn}}$.¹⁶ They observed a (2×1) reconstructed pattern for $P_{\text{Se}}/P_{\text{Zn}} \geq 2$ and a $c(2 \times 2)$ reconstructed surface for $P_{\text{Se}}/P_{\text{Zn}} \leq 1$. Farrell, deMiguel, and Tamargo showed that the Se-rich (2×1) structure converts to the Zn-rich $c(2 \times 2)$ structure through thermal desorption of Se for temperatures in the range 325–375 °C.¹⁷ They also reported an activation energy of 0.6 ± 0.1 eV for the electron-stimulated desorption of Se atoms from the ZnSe(100)- (2×1) surface.

In this paper, we study the dimer and vacancy-type structures on the ZnSe(100) surface and we calculate the thermodynamical stability of various surface reconstructions as a function of atomic chemical potential using a first-principles pseudopotential and local-density-functional formalism.²⁰ Since the (100) surface is polar, a theoretical determination of its atomic structures general-

ly requires the calculations of minimum-energy geometries as a function of Zn or Se coverage, or equivalently as a function of Zn or Se chemical potentials.^{10–14} By determining the surface energies as a function of the Zn chemical potential (μ_{Zn}), we can compare the energies of structures with different stoichiometries. For each value of μ_{Zn} , within an allowed range, we determine the structure having the lowest formation energy. We examine both Zn- and Se-terminated surfaces with surface coverages Θ of 1, $\frac{1}{2}$, $\frac{3}{4}$, and $\frac{1}{4}$ and concentrate principally on the (2×1) , (1×2) , $c(2 \times 2)$, and (4×2) reconstructed structures.

The electron counting rule is helpful in understanding the surface reconstructions of polar semiconductors.²¹ Ordinarily nonmetallic surfaces are energetically favorable with respect to metallic surfaces even for nonpolar semiconductors. For example, the Si(100) surface has a well-known (2×1) -dimer reconstruction, and four electrons per 2×1 cell take part in dimerization. The dimer formation leads to the bonding $pp\sigma$ and $pp\pi$ states in a tight-binding picture. The surface is semimetallic for the symmetric dimerization because of an overlap of the bonding $pp\pi$ and antibonding $pp\pi^*$ bands, but becomes nonmetallic through an asymmetric buckling of the dimers.^{5,6} Alternative vacancy structures are known to be nonmetallic, but are metastable with respect to the dimerized surface.

For GaAs(100) surfaces, the simple (2×1) -dimer structures for full surface coverage ($\Theta=1$) for either the Ga- or As-(100) surface is metallic, since three or five electrons take part in the dimerization, respectively, and the odd number of electrons makes the surface metallic. Thus, complex structures arising from combinations of dimers and vacancies are required to make the surface stable and nonmetallic. The GaAs(100) surface exhibits a multitude of reconstructions, often with large unit cells, as a function of surface stoichiometry and temperature.^{9–11,22–25}

For a II-VI semiconductor such as ZnSe, each cation has two valence electrons, and each anion has six valence electrons, thus on average, each atomic orbital contributes $\frac{1}{2}$ or $\frac{3}{2}$ electrons to each bond in the zinc-blende

structure. There are thus one (i.e., $2 \times \frac{1}{2}$) or three (i.e., $2 \times \frac{3}{2}$) electrons in the two dangling bonds per cation or anion on the ideal (1×1) cation- or anion-terminated (100) surfaces. Unlike the case of III-V surfaces, dimerization can make each surface nonmetallic. Thus, the simple dimer structures for the cation- or anion-terminated surfaces are expected to be at least metastable structures for II-VI semiconductors. Since only two electrons make up a σ bond for the Zn-dimer structure, the strength of the bond is expected to be weaker than that of a Si dimer where both $pp\sigma$ and $pp\pi$ interactions contribute to the bond strength. For the case of a Se dimer, six electrons take part in the dimer bond, and these occupy the $pp\pi^*$ antibonding state, in addition to the $pp\sigma$ and $pp\pi$ bonding states. The strength of the dimer bond for the Se dimer is also expected, therefore, to be weaker than that of the Si dimer.

In addition to the dimer structures, the vacancy structures corresponding to a surface coverage of $\Theta = \frac{1}{2}$ also make the surface electronic structure nonmetallic. This occurs because the dangling bonds on the anions accept electrons from the dangling bonds on the cations and become fully occupied. The large band gap and ionicity of some II-VI semiconductors such as ZnSe makes this electron exchange energetically very favorable. It is interesting, therefore, to test the stability of the dimer structures against the vacancy structures. We examine these issues in the following sections.

The paper is organized as follows. In Sec. II we describe the method of calculation. The results of the total-energy calculations for different reconstructions of Zn- and Se-terminated ZnSe(100) surfaces are discussed in Sec. III-VI, and the minimum-energy geometries as a function of chemical potential for ZnSe(100) surfaces are identified. A brief summary of the results is presented in Sec. VII.

II. METHOD OF CALCULATION

We use the first-principles pseudopotential total-energy²⁰ method within the local-density-functional approximation²⁶ in momentum space.²⁷ Norm-conserving nonlocal pseudopotentials are generated by the scheme proposed by Troullier and Martins²⁸ and the Kleinman-Bylander type of fully separable pseudopotentials²⁹ are constructed. Semirelativistic corrections to the ionic pseudopotentials are included.³⁰ The Ceperly-Alder correlation as parametrized by Perdew and Zunger is used.³¹ The wave functions are expanded in a plane-wave basis set with a kinetic-energy cutoff of 9 Ry. We do not consider $3d$ electrons explicitly for Zn atoms, and treat them as core because the surface reconstructions are mainly affected by the s and p valence electrons. Instead of it, we include partial core correction for Zn atoms.³²

To test the accuracy of the pseudopotentials, we calculate the total energy and the ground-state properties of bulk ZnSe. The calculated equilibrium lattice constant is 5.53 Å, which is only 2.6% smaller than the experimental value of 5.67 Å.³³ The calculated bulk modulus is 59.1 GPa, in good agreement with the experimental value of

62.5 GPa.³³ Four sampling k points for Brillouin-zone summations for a (2×2) cell and equivalent k -point sets for other unit cells are used. Since all the surfaces examined are nonmetallic, these k points are sufficient for comparisons of total energies. When nine sampling k points are used as a test for the Zn- $c(2 \times 2)$ structure, the difference in the total energies for the two sets of k points is within 0.08 eV/ (1×1) cell.

The surfaces are modeled by a slab geometry of nine atomic layers with a surface at each side plus a vacuum region equivalent to five atomic layers. We fix the lattice constant in the x - y plane parallel to the surface to the theoretical equilibrium value. The three central layers representing the bulk ZnSe are frozen throughout the calculation. Hellmann-Feynman forces³⁴ are calculated and the first, second, and third layers are relaxed until optimum atomic coordinates are established. Tests using different system sizes reveal that this approach works sufficiently well for the comparisons of energies of various surface structures.

To compare the total energies for surfaces with different stoichiometries, the stability of surfaces in an equilibrium with Zn and Se sources is considered and the chemical potentials are restricted within limits set by the free energies of the elemental *bulk* phases of Zn and Se. The surface energy σ may be expressed as

$$\sigma A = E_{\text{surface}} - n_{\text{Zn}}\mu_{\text{Zn}} - n_{\text{Se}}\mu_{\text{Se}}, \quad (1)$$

where E_{surface} is the calculated total energy of a ZnSe slab and A is the surface area of the slab. In addition, bulk ZnSe is a reservoir which can exchange atoms with the surface. If the surface is in equilibrium with the bulk, the sum of the chemical potentials is constrained to be equal to the energy of bulk ZnSe per Zn-Se pair.¹⁰ The maximum value for μ_{Zn} corresponds to $\mu_{\text{Zn}(\text{bulk})}$, and the minimum value corresponds to $\mu_{\text{Zn}(\text{bulk})} - \Delta H_f$ where ΔH_f is the heat of formation of bulk ZnSe from Zn and Se. *Ab initio* calculations of these bulk energies at $T=0$ K determine the limiting chemical potentials and also the heat of formation ΔH_f , which we calculate to be 1.62 eV per ZnSe, showing good agreement with the experimental value of 1.68 eV.³⁵ To calculate the total energy of bulk Zn, we use the experimentally observed hcp structure³⁶ and use a 75 k -point set. For the bulk Se, the hexagonal structure consisting of an aggregate of chains and a 39 k -point set is considered.³⁶

III. DIMERIZED SURFACES

A. Symmetry of dimers

The unreconstructed (1×1) structures for both Se- and Zn-terminated surfaces are found to be metallic and unstable with respect to dimerization. The asymmetric dimers with (2×2) unit cells are examined and found to be unstable with respect to the symmetric dimers for both Se and Zn surfaces. The results for the Zn and Se terminated surfaces are examined in the following.

B. Zn dimers

For the relaxed Zn-(1×1) structure, the highest occupied band arises from the dangling bond of surface Zn atoms and is located near the conduction band minimum. Dimerization lowers the total energy by 2.12 eV/dimer.

$$\Delta E_{\text{tot}}(\text{Zn dimer}) = -2.12 \text{ eV/dimer} . \quad (2)$$

This is larger than the dimerization energy of 1.68 eV/dimer for the Ga dimer on the GaAs(100) surface.¹⁰ The top view of the Zn-dimer (1×2) structure is shown in Fig. 1(a). The Zn-Zn bond length in the dimer bond is calculated to be 2.15 Å, smaller by about 21% as compared to that calculated in bulk metallic Zn. The atomic positions for the dimerized structure are summarized in Table I. The contours describing the charge densities for the Zn dimer are shown in Fig. 2(a). The figure is plotted in a plane which contains two-surface Zn atoms and two second-layer Se atoms. Most of the electrons are localized around Se atoms because of the strong ionicity. The electrons in the Zn-Zn dimer bonds are concentrated mostly at the center of the dimer, showing the covalent behavior of the σ bond. The shape of the contour graph of electron density is very similar to the case of a Ga dimer on the GaAs(100) surface.¹⁰ The highest occupied state associated with the Zn-dimer bond is calculated to be at about 1.0 eV above the valence-band maximum at the Γ point.

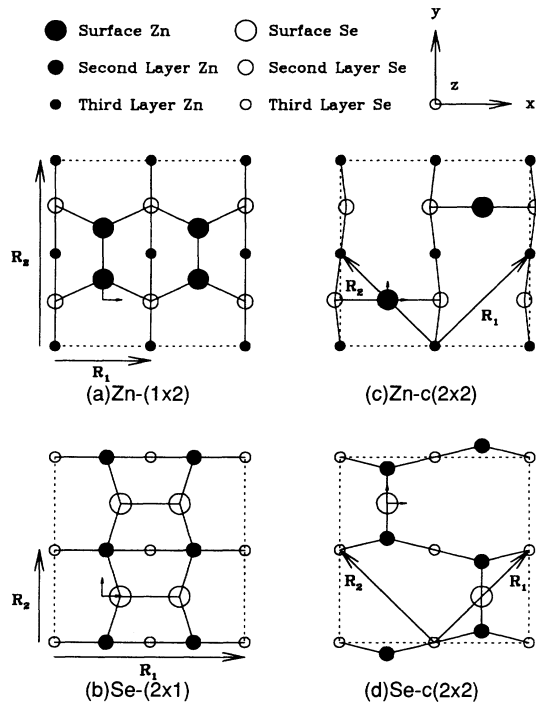


FIG. 1. Top views of reconstructed surfaces are shown: (a) Zn-terminated (1×2)-dimer structure; (b) Se-terminated (2×1)-dimer structure; (c) Zn-terminated $c(2\times 2)$ vacancy structure corresponding to $\Theta = \frac{1}{2}$; and (d) Se-terminated $c(2\times 2)$ vacancy structure with $\Theta = \frac{1}{2}$. Solid circles represent Zn atoms, and open circles Se atoms. The R_1 and R_2 indicate the lattice vectors of unit cells.

C. Se dimers

For the (2×1) Se-dimer structure, the dimerization of the (1×1) structure lowers the energy by 1.08 eV/dimer,

$$\Delta E_{\text{tot}}(\text{Se dimer}) = -1.08 \text{ eV/dimer} , \quad (3)$$

which is smaller than the dimerization energy of the Zn dimer but larger than the dimerization energy of 0.60 eV/dimer for the As dimer on the GaAs(100) surface.¹⁰ The top view of a Se-dimer (2×1) structure is shown in Fig. 1(b). The Se-Se bond length is 2.40 Å, nearly the same as that calculated for bulk metallic Se. The atomic positions for the dimerized structure are summarized in Table I. The charge densities for the Se dimer are shown in Fig. 2(b). The figure is plotted in a plane which contains two-surface Se atoms and two second-layer Zn atoms. The electrons in the Se-Se dimer bond show the behavior of π bonds. The shape of the contour graph for the electron density is very similar to that for the As dimer on the GaAs(100) surface.¹⁰ There are three states associated with the Se-dimer bond. All are occupied and are located near the valence-band maximum. The highest one is calculated to be at about 0.4 eV above the valence-band maximum at the Γ point and the other bands are calculated to lie below the valence-band maximum.

TABLE I. Surface atomic coordinates for the dimerized and vacancy structures. Refer to Fig. 1 for the Cartesian coordinate system. The origin of the coordinate system is taken to be at the position of a surface Zn(Se) atom on the ideal 1×1 surface. All numbers are in units of $\sqrt{2}a_0$. The calculated value of 5.53 Å is used for the ZnSe lattice constant a_0 .

	x	y	z
Zn-dimer (1×2)			
Surface Zn	0.0	0.0+0.1123	-0.0481
Second layer Se	0.25	0.0-0.0096	$\frac{1}{4\sqrt{2}}$ -0.0026
Third layer Zn	0.25	-0.25	$\frac{1}{2\sqrt{2}}$ -0.0037
	0.25	0.25	$\frac{1}{2\sqrt{2}}$ +0.0006
Se-dimer (2×1)			
Surface Se	0.0+0.0967	0.0	0.0041
Second layer Zn	0.0+0.0277	0.25	$\frac{1}{4\sqrt{2}}$ +0.0048
Third layer Se	-0.25	0.25	$\frac{1}{2\sqrt{2}}$ +0.0331
	0.25	0.25	$\frac{1}{2\sqrt{2}}$ -0.0191
Zn-c(2×2)			
Surface Zn	0.0	0.0	-0.1635
Second layer Se	0.25+0.0294	0.0	$\frac{1}{4\sqrt{2}}$ +0.0021
Third layer Zn	0.25	0.25	$\frac{1}{2\sqrt{2}}$ -0.0012
Se-c(2×2)			
Surface Se	0.0	0.0	0.0074
Second layer Zn	0.0	0.25-0.0621	$\frac{1}{4\sqrt{2}}$ -0.0235
Third layer Se	0.25	0.25	$\frac{1}{2\sqrt{2}}$ -0.0104

IV. VACANCY-TYPE RECONSTRUCTIONS

A. Structure

We consider three possibilities for the vacancy structures with a half-monolayer coverage ($\Theta = \frac{1}{2}$): (i) a (2×1) or (1×2) structure; (ii) a $c(2 \times 2)$ structure; and (iii) a (2×2) -dimer-vacancy configuration. Among these the $c(2 \times 2)$ structures are found to be the most stable, the (2×1) or (1×2) structure is metastable for Zn- and Se-terminated surfaces, and the (2×2) -dimer-vacancy configurations are unstable. Although the lattice relaxation can be better accommodated in the (2×1) or (1×2) vacancy structure than the $c(2 \times 2)$ structures, the elec-

trostatic interactions between the dangling bonds of Zn and Se atoms on the vacancy reconstructed surfaces arising from charge transfer make the $c(2 \times 2)$ structure the most favorable structure. In the following, we describe our results for the Zn- and Se-terminated surfaces for $\Theta = \frac{1}{2}$.

B. Zn vacancies

For the vacancy structure on the Zn(100) surface, the electrons in the dangling bonds of the surface Zn atoms are transferred into the dangling bonds of the second-layer Se atoms. The surface Zn atoms relax towards the second-layer Se atoms and the Se-Zn-Se bond angle be-

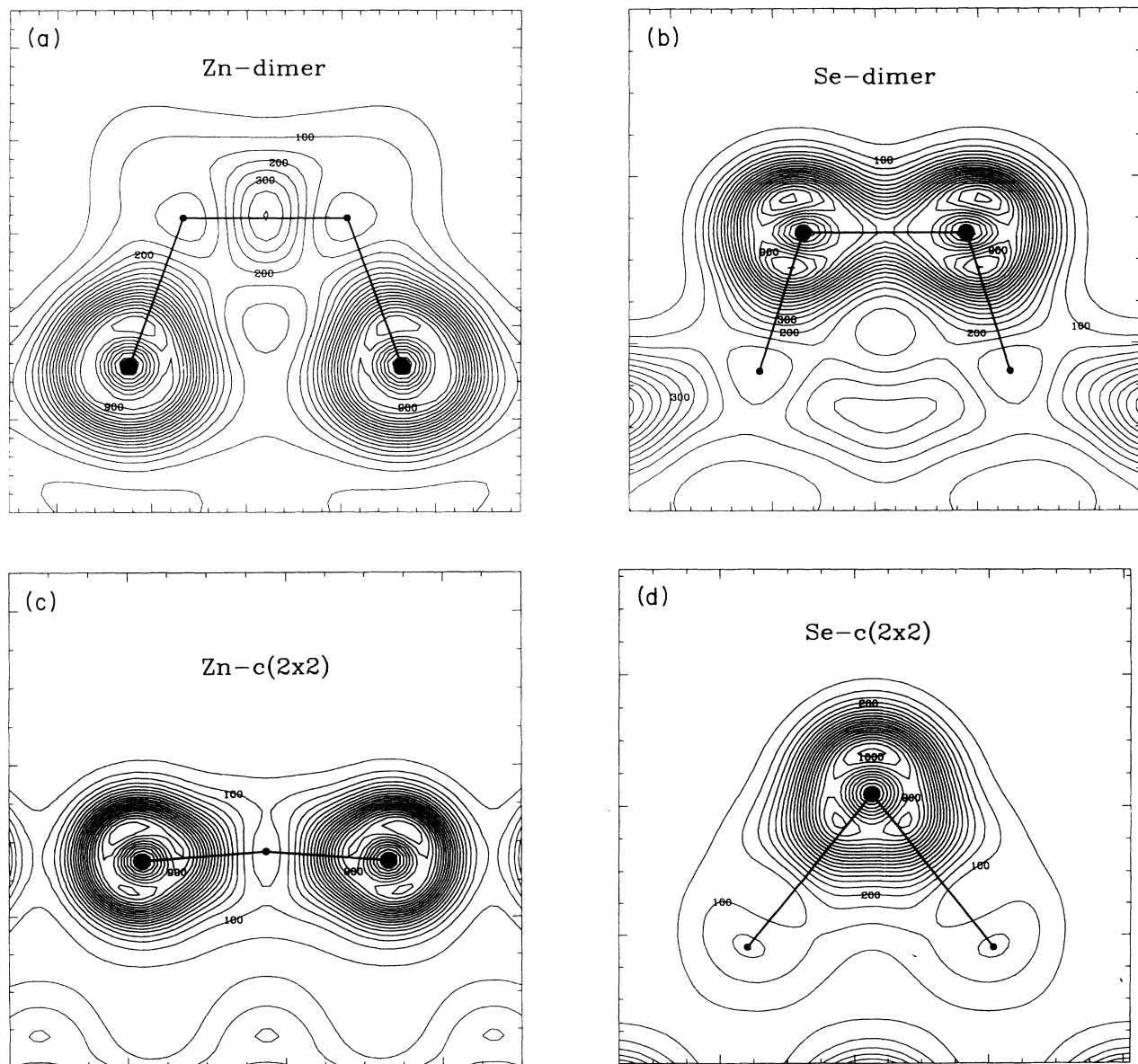


FIG. 2. Charge-density contour plots for ZnSe(100) surfaces: (a) Zn (1×2) -dimer structure; (b) Se (2×1) -dimer structure; (c) Zn- $c(2 \times 2)$ vacancy structure; (d) Se- $c(2 \times 2)$ vacancy structure. Large solid circles denote Se atoms, and small circles Zn atoms. Units are electrons/supercell with a spacing of 50; the volume of the supercells is 1182.5 \AA^3 .

comes nearly 180° , i.e., the surface Zn atoms become coplanar with the subsurface Se atoms. The (2×1) Zn-vacancy structure is less stable, by $0.02 \text{ eV}/(1 \times 1)$ cell, than the $c(2 \times 2)$ vacancy structure shown in Fig. 1(c). Since all the electrons in the Zn dangling bonds empty into the Se dangling bonds, no electrons are left for the dimerization. The Zn-Se bond length at the surface is 2.19 \AA and is compressed by 8.7% compared to the ideal bulk distance. The reduction in the bond length occurs as a result of the charge transfer and the reduced coordination of the cation.³⁷ The atomic positions for the Zn- $c(2 \times 2)$ structure are summarized in Table I.

The charge density for the Zn- $c(2 \times 2)$ structure is shown in Fig. 2(c). The figure is plotted in a plane which contains a surface Zn atom and two second-layer Se atoms. The electron density is similar to that of the Ga-vacancy structure on the GaAs(100) surface.¹⁰ The electrons around the relaxed Zn atoms form an sp type of hybridization. The energy-level positions of the surface states due to the dangling bond states of Se atoms which contribute two states per the (2×1) cell lie below the valence-band maximum at the Γ point.

C. Se vacancies

For the case of the Se-vacancy structure, the electrons in the dangling bonds of the Zn atoms in the second layer are transferred to the dangling bonds of the Se atoms in the surface layer and fill the dangling-bond states of the Se atoms. All orbitals are totally full for the Se-vacancy structure, and this prevents dimerization of the Se atoms. The extra electrons around the surface Se atoms is found to reduce the Zn-Se-Zn angle to 82° which is appreciably smaller than the ideal bond angle of 109° in the zincblende structure. The loss of electrons around the Zn atoms in the second layer makes each subsurface Zn atom become coplanar with its three Se nearest neighbors. The sum of the three bond angles around this Zn atom is 356° , which shows that the subsurface Zn atoms make sp^2 -like bonds with Se atoms. The Se-Zn bond length at the surface is reduced to 91.5% of its bulk value, and becomes 2.19 \AA . The shrinking of the bond length is a direct consequence of the charge transfer between the atoms. The (1×2) Se-vacancy structure is less stable, by $0.01 \text{ eV}/(1 \times 1)$ cell, than the $c(2 \times 2)$ Se-vacancy structure in Fig. 1(d). The atomic positions for the $c(2 \times 2)$ structure are summarized in Table I.

The charge densities for the Se vacancy are shown in Fig. 2(d). The figure is plotted in a plane which contains a surface Se atom and two second-layer Zn atoms. The dangling bonds of the surface Se atoms are "overpopulated" by electrons, occupied by four electrons, and the highest occupied state corresponding to an antibonding $pp\pi^*$ Se-dangling-bond state lie near the conduction-band minimum.

V. STABILITY OF SURFACES

Since the number of Zn and Se atoms can be made to be the same for the Zn-vacancy and Se-vacancy structures, we can compare directly the surface energies for

the $\Theta = \frac{1}{2}$ surfaces without any need for considering the atomic chemical potentials. In fact, the absolute surface formation energies for the vacancy structures can be determined from the increase in the total energy above that of bulk ZnSe with an equivalent number of Zn and Se atoms.

For $\Theta = \frac{1}{2}$, the surface energy of the Se-vacancy structure [$0.65 \text{ eV}/(1 \times 1)$ cell] is larger than that for the Zn-vacancy structure [$0.38 \text{ eV}/(1 \times 1)$ cell]. The difference amounts to $0.27 \text{ eV}/(1 \times 1)$ cell in favor of the Zn-vacancy structure. The Se-vacancy structure has twice as many dangling bonds than the Zn-vacancy structure. Usually the reconstruction minimizing the number of dangling bonds per surface atom is more stable.

For other stoichiometries, the surface energies under equilibrium conditions can be compared only when atomic exchange with either Zn or Se reservoirs is considered. The surface energy in Eq. (1) may be written¹⁰

$$\sigma A = E_{\text{surface}} - \frac{1}{2}(\mu_{\text{Zn}} + \mu_{\text{Se}})n_{\text{tot}} + \frac{1}{2}(\mu_{\text{Zn}} - \mu_{\text{Se}})\Delta n, \quad (4)$$

where $n_{\text{tot}} = n_{\text{Se}} + n_{\text{Zn}}$ and $\Delta n = n_{\text{Se}} - n_{\text{Zn}}$. The sum of chemical potentials in the second term is set to $\mu_{\text{ZnSe(bulk)}}$, while the allowed range of the difference in chemical potentials in the third term is

$$-\Delta H_f \leq (\mu_{\text{Zn}} - \mu_{\text{Se}}) - (\mu_{\text{Zn(bulk)}} - \mu_{\text{Se(bulk)}}) \leq \Delta H_f. \quad (5)$$

The surface energies for various structures as a function of Δn are compared in Fig. 3. The allowable range of the

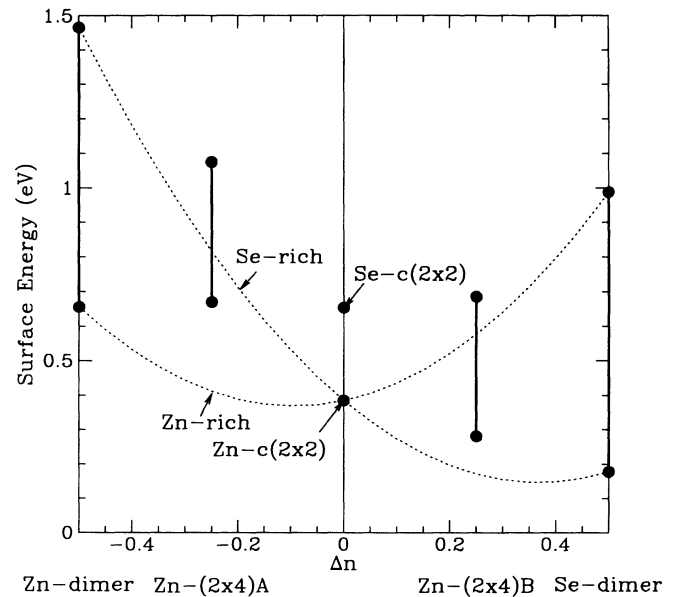


FIG. 3. Surface formation energies $E_{\text{formation}} = E_{\text{surface}} - \sum \mu_i n_i$ per (1×1) unit cell as a function of $\Delta n = (n_{\text{Se}} - n_{\text{Zn}})$. The points are the calculated values for the limiting cases of Zn-rich and Se-rich chemical potentials. Solid lines represent the surface energies for the intermediate chemical potentials. The dotted curves are the parabolic fits through the points shown as a guide to the energies of other possible structures with different stoichiometries. The area between the two curves represents a region of the intermediate chemical potentials.

surface energies for the filled Se and Zn surfaces are shown by solid lines according to Eqs. (4) and (5). We use the calculated value for ΔH_f . We have also drawn the parabolic fits to the calculated points, which would represent the surface energies of other possible off stoichiometric surfaces.

In Fig. 4, we compare the surface energies as a function of the chemical potential of the Zn reservoir by using Eq. (1), in which the range of μ_{Zn} is chosen to be between $\mu_{Zn(\text{bulk})} - \Delta H_f$ and $\mu_{Zn(\text{bulk})}$ and μ_{Se} is $\mu_{ZnSe(\text{bulk})} - \mu_{Zn}$. The surface energy of the Zn- $c(2 \times 2)$ structure is taken as a reference value in Fig. 4. Only two types of structures are energetically favorable among the considered structures. The Se-dimer (2×1) structure is favorable in the region of low μ_{Zn} , i.e., Se-rich condition, while the Zn vacancy $c(2 \times 2)$ structure is favorable in the region of high μ_{Zn} , i.e., Zn-rich condition. These results are in good agreement with the experimental facts that only two types of Zn- $c(2 \times 2)$ and Se-dimer (2×1) structures have been observed for the Zn-rich and Se-rich conditions, respectively.¹⁵⁻¹⁹ We find that the formation of the Zn-vacancy structure by the removal of Zn atoms from the Zn-dimer structure of $\Theta = 1$ is exothermic in any region of μ_{Zn} . The Se- $c(2 \times 2)$ structure can be favorable relatively to the Se-dimer (2×1) structure in the Zn-rich conditions, but unstable to the Zn- $c(2 \times 2)$ structure.

As discussed earlier, for a $\Theta = \frac{1}{2}$ Zn-terminated surface, the electrons around the surface Zn atoms form an sp -type hybridization for the vacancy structure. Generally sp -type hybridization is more stable than sp^2 - and sp^3 -type hybridization. The energy reduction by this type of hybridization may make the Zn-vacancy structure stable relative to the Zn-dimer structure. In addition, since only two electrons take part in the Zn-Zn dimerization forming a σ bond, the energy reduction from the dimeri-

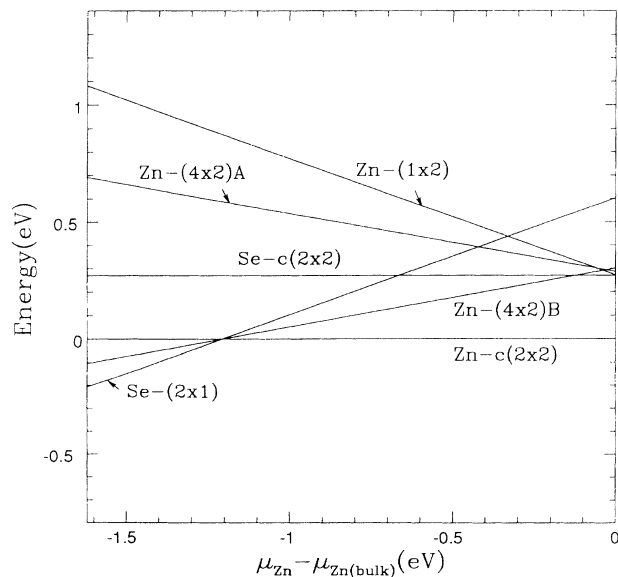


FIG. 4. Surface formation energies per (1×1) unit cell for ZnSe(100) surfaces as a function of μ_{Zn} over the thermodynamically allowed range: $-\Delta H_f \leq \mu_{Zn} - \mu_{Zn(\text{bulk})} \leq 0$. We use the calculated value for $-\Delta H_f$.

zation is not large and the dimerization is not favorable relatively to the vacancy formation. For the Se-terminated surface, the surface Se atoms in the vacancy structure have many dangling-bond states, which make the vacancy formation unfavorable relatively to the dimer formation.

VI. (4×2) SURFACES: COMBINED VACANCY-DIMER STRUCTURES

We have also examined the (4×2) reconstructed surfaces with various combinations of dimers and vacancies with $\Delta n = -\frac{1}{4}$ or $\frac{1}{4}$, since the surfaces of $\Delta n = \frac{1}{4}$ or $-\frac{1}{4}$ may be stable structures, considering the parabolic curves in Fig. 3. For the Zn-terminated (4×2) surface, we consider two types of nonmetallic structure. The Zn- $(4 \times 2)A$ structure shown in Fig. 5(a) is a combination of Zn vacancies and Zn dimers, and its surface coverage Θ is $\frac{3}{4}$ corresponding to $\Delta n = -\frac{1}{4}$. The other type of nonmetallic surface results from a combination of Se dimers and Zn vacancies shown as the Zn- $(4 \times 2)B$ structure in Fig. 5(b). This surface has a stoichiometry of $\Delta n = \frac{1}{4}$. This structure is expected to be stable in an intermediate condition between the chemical potentials for which the Se-dimer or Zn- $c(2 \times 2)$ structure is stable. For a Se-terminated (2×4) surface, the structure similar to Fig. 5(a) is a combination of Se vacancies and Se dimers, and the structure similar to Fig. 5(b) is a combination of Se vacancies and Zn dimers. Since the surface energy of Se-vacancy structures is larger than that of Zn-vacancy structure, these Se- (2×4) structures are expected to be unfavorable as compared to the Zn- (4×2) structures.

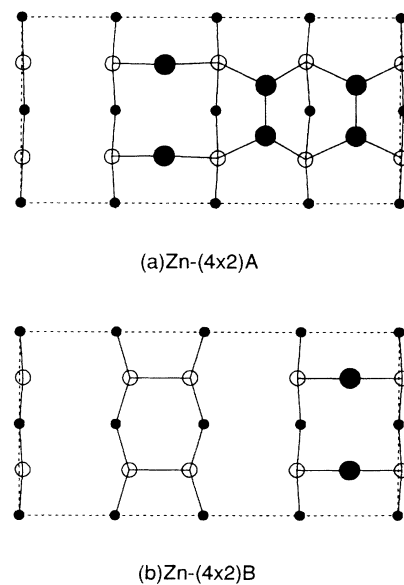


FIG. 5. Top views of two types of Zn-terminated (4×2) reconstructions: (a) Zn- $(4 \times 2)A$ surface with coverage $\Theta = \frac{3}{4}$, which consists of Zn vacancies and Zn dimers; and (b) Zn- $(4 \times 2)B$ surface with $\Theta = \frac{1}{4}$, which consists of Zn-vacancies and Se dimers. Solid circles denote Zn atoms, and open circles Se atoms.

Therefore, we do not consider Se-(2×4) structures in this work.

The calculated surface energies for the Zn-terminated (4×2) structures are indicated in Figs. 3 and 4. The surface energies are larger than the values fitted by parabolic curves in Fig. 3. A Zn-(4×2)*A* surface is unstable with respect to the Zn-*c*(2×2) structure for all values of Zn-chemical potential, as shown in Fig. 4, although it is more stable than a Zn-dimer (1×2) structure for most values of μ_{Zn} . It is a very small region that the Zn(4×2)*B* structure is stable or metastable, although the formation of the Zn-(4×2)*B* structure is more favorable than Zn-dimer, Zn-(4×2)*A*, and Se-vacancy structures.

VII. SUMMARY

We have presented the results of total-energy calculations for the Zn- and Se-terminated (1×2), (2×1), *c*(2×2), and Zn-terminated (4×2) reconstruction structures on the ZnSe(100) surface, and compared the surface energies between different stoichiometric structures in the

context of a thermodynamic model. The (1×1) structures for both Se- and Zn-terminated surfaces are unstable with respect to dimerization. The Zn-Zn dimer bond energy of 2.12 eV/dimer is appreciably larger than the Se-Se dimer bond energy of 1.08 eV/dimer. For the coverage $\Theta = \frac{1}{2}$ vacancy structures, the *c*(2×2) structures are more stable than the (2×1) or (1×2) structure for both Zn- and Se-terminated surfaces, and the dimer-vacancy models are unstable. When atomic exchanges with bulk Zn or Se reservoirs are considered, a Zn-vacancy *c*(2×2) structures is found to be the most favorable for the Zn-terminated surface under a Zn-rich condition, while a Se-dimer (2×1) structure is the most favorable for the Se-terminated surface under a Se-rich condition.

ACKNOWLEDGMENTS

We would like to thank Professor A. Kahn, Weidong Chen, Dr. Amy Liu, and Dr. N. Troullier for helpful discussions.

- ¹M. A. Haase, J. Qiu, J. M. DePuydt, and H. Cheng, *Appl. Phys. Lett.* **59**, 1272 (1991).
- ²H. Jeon, J. Ding, A. V. Nurmikko, W. Xie, D. C. Grillo, M. Kobayashi, R. L. Gunshor, G. C. Hua, and N. Otsuka, *Appl. Phys. Lett.* **60**, 2045 (1992).
- ³J. Qiu, J. M. Depuydt, H. Cheng, and M. A. Hasse, *Appl. Phys. Lett.* **59**, 2992 (1991).
- ⁴For a review, see, e.g., *Rep. Prog. Phys.* **50**, 1045 (1987), and references cited therein.
- ⁵D. J. Chadi, *Phys. Rev. Lett.* **43**, 43 (1979); *J. Vac. Sci. Technol.* **16**, 1290 (1979).
- ⁶J. E. Northrup, *Phys. Rev. B* **47**, 10032 (1993).
- ⁷I. Stich, M. C. Payne, R. D. King-Smith, J.-S. Lin, and L. J. Clarke, *Phys. Rev. Lett.* **68**, 1351 (1992).
- ⁸K. D. Brommer, M. Needels, B. E. Larson, and J. D. Joannopoulos, *Phys. Rev. Lett.* **68**, 1355 (1992).
- ⁹D. J. Chadi, *J. Vac. Sci. Technol. A* **5**, 834 (1987); G.-X. Qian, R. M. Martin, and D. J. Chadi, *Phys. Rev. Lett.* **60**, 2176 (1988).
- ¹⁰Gui-Xin Qian, R. M. Martin, and D. J. Chadi, *Phys. Rev. B* **38**, 7649 (1988).
- ¹¹John E. Northrup and Sverre Froyen, *Phys. Rev. Lett.* **71**, 2276 (1993).
- ¹²E. Kaxiras, K. C. Pandey, Y. Bar-Yam, and J. D. Joannopoulos, *Phys. Rev. Lett.* **56**, 2819 (1986).
- ¹³E. Kaxiras, Y. Bar-Yam, J. D. Joannopoulos, and K. C. Pandey, *Phys. Rev. B* **33**, 4406 (1986).
- ¹⁴E. Kaxiras, Y. Bar-Yam, J. D. Joannopoulos, and K. C. Pandey, *Phys. Rev. Lett.* **57**, 106 (1986).
- ¹⁵K. Menda, I. Takayasu, T. Minato, and M. Kawashima, *Jap. J. Appl. Phys.* **26**, L1326 (1987).
- ¹⁶K. Menda, T. Minato, and M. Kawashima, *Jpn. J. Appl. Phys.* **28**, 1560 (1989).
- ¹⁷H. H. Farrell, J. L. deMiguel, and M. C. Tamargo, *J. Appl. Phys.* **65**, 4084 (1989).
- ¹⁸M. Vos, F. Xu, S. G. Anderson, J. H. Weaver, and H. Cheng, *Phys. Rev. B* **39**, 10744 (1989).
- ¹⁹T. Yao, Z. Q. Zhu, K. Uesugi, S. Kamiyama, and M. Fujimoto, *J. Vac. Sci. Technol. A* **8**, 997 (1990).
- ²⁰M. L. Cohen, *Phys. Scr.* **T1**, 5 (1982).
- ²¹M. D. Pashley, *Phys. Rev. B* **40**, 10481 (1989).
- ²²J. R. Arthur, *Surf. Sci.* **43**, 449 (1974).
- ²³A. Y. Cho, *J. Appl. Phys.* **47**, 2841 (1976).
- ²⁴K. Larsen, J. H. Neave, and B. A. Joyce, *J. Phys. C* **14**, 167 (1981).
- ²⁵R. Z. Bachrach, *Progress in Crystal Growth and Characterization* (Pergamon, London, 1979), Vol. 2, pp. 115–144; R. Z. Bachrach *et al.*, *J. Vac. Sci. Technol.* **18**, 797 (1981).
- ²⁶P. Hohenberg and W. Kohn, *Phys. Rev.* **136**, B864 (1964); W. Kohn and L. J. Sham, *ibid.* **140**, A1133 (1965).
- ²⁷J. Ihm, A. Zunger, and M. L. Cohen, *J. Phys. C* **12**, 4409 (1979).
- ²⁸N. Troullier and J. L. Martins, *Phys. Rev. B* **43**, 1993 (1991).
- ²⁹L. Kleinman and D. M. Bylander, *Phys. Rev. Lett.* **48**, 1424 (1982).
- ³⁰G. B. Bachelet and M. Schlüter, *Phys. Rev. B* **25**, 2103 (1982); L. Kleinman, *ibid.* **21**, 2630 (1980).
- ³¹P. M. Ceperly and B. J. Alder, *Phys. Rev. Lett.* **45**, 566 (1980); J. P. Perdew and A. Zunger, *Phys. Rev. B* **23**, 5048 (1981).
- ³²S. G. Louis, S. Froyen, and M. L. Cohen, *Phys. Rev. B* **26**, 1738 (1982).
- ³³*Landolt-Börnstein Tables*, edited by O. Madelung, M. Schulz, and H. Weiss (Springer, Berlin, 1984), Vol. 17a, and references therein.
- ³⁴H. Hellmann, *Einführung in die Quanten Theorie* (Deuticke, Leipzig, 1937), p. 285; R. P. Feynman, *Phys. Rev.* **56**, 340 (1939).
- ³⁵*Handbook of Chemistry and Physics*, 73rd ed., edited by D. R. Lide (CRC, Boca Raton, 1992).
- ³⁶Ralph W. G. Wyckoff, *Crystal Structures* (Wiley, New York, 1963).
- ³⁷C. Kittel, *Introduction to Solid State Physics*, 6th ed. (Wiley, New York, 1986), p. 77.